Fabrication of 30-nm-scale structures for electron transport studies using a polymethylmethacrylate bilayer resist

M. J. Rooks, S. Wind, P. McEuen, and D. E. Prober
Yale University, Section of Applied Physics, P.O. Box 2157, Yale Station, New Haven, Connecticut 06520

(Received 6 June 1986; accepted 6 October 1986)

We describe a polymethylmethacrylate (PMMA) bilayer system which provides a simple high-resolution resist for the research and development of structures smaller than ~ 0.2 μm. Intermixing between the two resist layers is avoided by the use of a weak solvent, xylene, as the solvent of the upper PMMA layer. Metal lines as narrow as 30 nm have been fabricated for electron-transport studies. Much larger features can be produced with deep-ultraviolet exposure, which facilitates electrical contact to the ultrasmall structures.

I. INTRODUCTION

The demands of large-scale integration have driven forward research in microfabrication, particularly in microlithography. The need for reliable micron scale patterning has led to the development of multilayer optical resists. The requirements of nanometer-scale device studies have created a similar need for high-resolution e-beam resists. A number of articles have reviewed progress on "nanometer-scale" fabrication methods.[1–7] As features approach the nanometer size scale, new quantum phenomena become significant. Quantum corrections to the electrical conductivity, electron quantum-interference phenomena, and conductance fluctuations are being studied in a number of laboratories.[8,9]

The lithography used for nanometer-scale studies must not only produce features smaller than 100 nm, but must also work reliably with a variety of materials. It is also often important that the e-beam patterning process be compatible with some form of optical lithography, so that large features (i.e., contact pads) can be fabricated simultaneously. When the required resolution of e-beam lithography is in the ~ 10 nm range, a multilayer approach is often desirable, especially if the exposure system has only moderate resolution. Many of the e-beam multilayer approaches are similar to those of optical lithography; also, the same types of problems are encountered. This paper describes a specific e-beam multilayer resist process which uses one of the more recent, and more promising, multilayer techniques.

There are numerous process requirements which motivate the use of multilayer resists.[10] High resolution patterning is best achieved through the use of a thin imaging layer. However, good step coverage over existing features, and an undercut profile for liftoff processing,[3,11] are best achieved through the use of a thicker lower layer.

The typical problem encountered with a multilayer resist approach is that the two resist layers may intermix. In addition to reducing the effectiveness of either layer, the thin intermixed layer can prevent proper exposure or development of the bottom layer.[10] The intermixing between resist layers can be eliminated by using materials which do not react with each other or with the solvent of the other layer.

Significant bilayer resist techniques for e-beam lithography have been presented by Hatzakis and co-workers.[11] One such process uses a bilayer consisting of a layer of PMMA and a layer of a copolymer, poly (methylmethacrylate/methacrylic acid). The solvent used for each layer does not dissolve the other layer. For high sensitivity (low exposure dose) the copolymer is the top (imaging) layer.[11] For high resolution, PMMA is used as the imaging layer.[3] This latter bilayer system has produced metal lines as narrow as 35 nm with an SEM exposure system. Narrower linewidths can presumably be achieved with a higher resolution exposure system.

The bilayer process described in this paper was developed at the University of Glasgow.[5] Our PMMA/PMMA bilayer consists of two layers of PMMA of different molecular weights, with the higher molecular weight (lower sensitivity) polymer as the top layers (see Fig. 1, inset). Both layers are exposed with a single exposure, and then developed with one development step.

In this paper we present the details of the PMMA/PMMA bilayer process, some of which are not available in Ref. 5. This bilayer resist is now being used to produce patterns for various studies of device physics and electron transport, and has proven to be reliable and versatile.

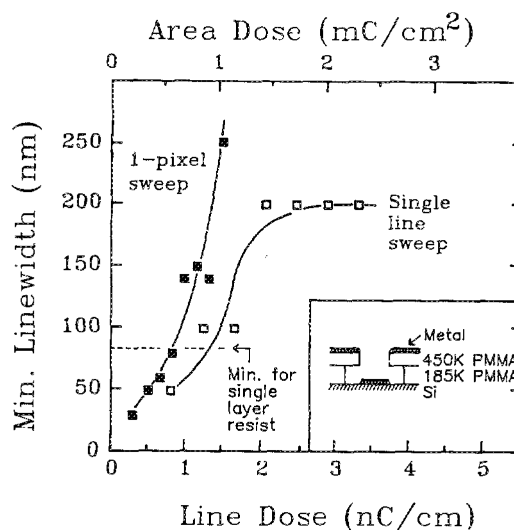

FIG. 1. Minimum linewidth vs dose of metal lines after liftoff for the PMMA/PMMA bilayer system. Area dose applies only for the 1-pixel wide sweep; the width of the 1-pixel sweep is 15 nm = (field size)/1024. (Area Dose) = (Line Dose)/15 nm. Inset: bilayer resist profile with evaporated metal.

 © 1987 American Vacuum Society

II. TECHNIQUES AND PROCESSING

The PMMA/PMMA bilayer uses a sensitive bottom layer of PMMA (molecular weight 185 K) covered with a less sensitive top layer of PMMA (molecular weight 450 K). The resist structure is shown in the inset of Fig. 1, and the processing steps are outlined in Table I. The solubility of PMMA in developer is greater for a lower molecular weight. As a result the bottom layer is approximately 1.5 times more sensitive[5] than the top layer, so that upon development the bilayer forms an undercut profile, as shown in Fig. 1. An undercut profile is desirable since we use the liftoff technique to pattern the metal film.

The resist solvent must be chosen carefully in order to avoid mixing of the layers. If a solution of PMMA in chlorobenzene (the solvent commonly used) is spun on top of a baked layer of PMMA, the chlorobenzene partially dissolves the bottom layer. To avoid this we have used xylene as the solvent for the top layer, since xylene is only a very weak solvent for PMMA. Most of the xylene evaporates from the top layer before any significant part of the bottom layer is dissolved. (Mixing due to subsequent thermal inter-diffusion appears to be negligible.) The two layers of PMMA are developed at one time with the same weak developer [1:3 methyl isobutyl ketone: isopropanol (MIBK: IPA)], so that any small inter-diffused layer simply forms a thin region of intermediate sensitivity. The lack of intermixing is indicated by the liftoff properties of the bilayer, which are significantly better than those of a single PMMA layer of the same total thickness. We note that xylene is less toxic than chlorobenzene.

The resist layers are spun on as solutions of $\sim 3\%$ solids for both molecular weights. These are prepared by stirring the mixtures in closed glass containers with a magnetic stirrer. Since xylene is an inefficient solvent, it is necessary to stir for 24 h at a temperature of 60 °C. Resist solutions are stored at room temperature and show no signs of precipitation.

Thicknesses of single resist layers were measured for different spin speeds. The resist thickness was measured with a Dektak stylus machine with a resolution of 5 nm. Thicknesses of spun-on 450 K PMMA range between 92 nm for a spin speed of 2000 rpm to 45 nm at 8000 rpm. Thicknesses of the 185 K PMMA range between 65 nm at 2000 rpm to 32.5 nm at 8000 rpm. Both molecular weights of PMMA spin uniformly to $\pm 20\%$ over a 1.5 in. oxidized Si wafer. A similar measurement of thickness was made to determine the loss of unexposed resist due to a standard 30 s development in 1:3 MIBK:IPA at 23 °C (step 7 in the Table). The resist thickness loss was < 5 nm. An oxygen glow-discharge cleaning is used prior to metallization (step 10); the thickness loss due to this cleaning was also < 5 nm.

TABLE I. Processing steps.

Step	
(1)	Clean and oxidize silicon wafer
(2)	Spin 185 K PMMA, 3% in xylene, at 2500 rpm for 1 min (thickness ≈ 58 nm)
(3)	Bake for 1 h in air at 180°C
(4)	Spin 450 K PMMA, 3% in xylene, at 7000–9000 rpm for 1 min (thickness ≈ 40 nm).
(5)	Bake for 2 h in air at 180 °C
(6)	Expose with DUV using contact mask
(7)	Develop for 30 s in 1 : 3 MIBK:IPA, 23 °C
(8)	Expose with e-beam (see Fig. 1)
(9)	Develop for 30 s in 1 : 3 MIBK:IPA, 23 °C
(10)	Clean with oxygen glow discharge in evaporator
(11)	Evaporate metal
(12)	Liftoff by shooting acetone (see Ref. 5)

III. EQUIPMENT

Deep ultraviolet exposure (DUV) provides an efficient method of producing contact pads and large structures in the resist prior to e-beam exposure for fine-scale devices. In addition, the pattern left in the resist after DUV exposure and development can be used for alignment and focusing of the e-beam system. The bilayer resist is thus developed twice (see Table I), but the single layer of metal is lifted off in one step. An alternative approach would be to pattern separately two metal layers—the first for the leads and large-area structures, and the second for the fine-scale structures.[2,7] This alternate approach works well with gold for the large-area leads, since it does not oxidize or contaminate significantly. However, many devices (such as MOSFETs) require metals which can withstand high-temperature processing. Use of a gold film may be incompatible with such processes. Our two-exposure/two-development process allows a wide choice of materials and applications. The use of a liftoff process does, of course, restrict the substrate temperature during deposition.

PMMA can be exposed with light of wavelengths $\leqslant 240$ nm.[12] Our DUV contact exposure masks are made with chrome (thickness > 150 nm) or aluminum (thickness > 50 nm) on high-purity fused quartz plates. A mask aligner or a simple conformal exposure device[12] is used to provide hard contact between the mask and wafer. Two different light sources are used: a low-pressure mercury lamp (380 W), and a zinc lamp (7 W).[13] The zinc lamp produces almost no infrared radiation and so does not heat the wafer. Zinc has a strong spectral line at 214 nm, and thus is a far more efficient source. However, the zinc lamp is small, so the exposure is slow and is not uniform over large wafers. Neither of these DUV exposure sources is collimated. Exposure times with the mercury lamp are typically 45 min. The same exposure with the zinc lamp requires 3 h.

Electron beam exposure is done with a modified ISI SS-60 scanning electron microscope (SEM) with an electrostatic beam-blanker. The beam blanker and X–Y sweep are computer controlled, using a HP Series 200 computer and a custom interface built by our research group. An X–Y raster pattern is utilized. Patterns are mapped onto a grid of 1024 $\times$ 1024 pixels. The raster speed is controlled from software. The raster speed is increased in the unexposed regions of the pattern. For typical patterns this reduces the exposure time by a factor of 2 to 5 compared to that which would be obtained with a single raster speed. A software controlled settling time allows the scan coils to settle when switching raster speeds. Proximity effect corrections are not included in the present design, but could be added.

The typical exposure field is $15 \times 15\,\mu$m, for a pixel size of

15×15 nm. Each pixel in the pattern is exposed with four single-line horizontal sweeps whose line centers are offset by 3.7 nm (1/4 pixel) between each sweep. For tests of minimum achievable linewidths, we employ exposures either one pixel (four sweeps) wide, or 1/4 pixel (one sweep) wide. The beam energy commonly used is 30 keV, and the beam current used for a 15 μm×15 μm field is 15 pA.

IV. LITHOGRAPHY RESULTS

Figure 1 shows our result for linewidth of metal lines versus dose for the bilayer resist. Linewidths are measured with a JEOL 100CX in the SEM mode. Measured linewidths are consistent with electrical measurements on several samples. The minimum linewidth achieved is 30 nm. The single-line exposure and the 1-pixel-wide exposure produce comparable linewidths. Figure 1 shows that the 1-pixel sweep produced a narrower minimum linewidth in this particular test. A single-line sweep can apparently produce a 30 nm wide line as well, although this may require tighter control of processing parameters than for the 1-pixel-wide exposure.

We find that with a *single-layer* PMMA resist, we can produce lines only as narrow as 70 to 80 nm with the same exposure system. In addition, with the single-layer resist, proper liftoff often requires ultrasonic agitation, so that the choice of patterned materials is more restricted. We also find that the linewidths achieved using the bilayer resist are more reproducible than those using the single-layer resist.

Figure 2 shows a TEM micrograph of the PMMA/PMMA bilayer resist profile. Samples for TEM studies are prepared by spinning the bilayer on a substrate of polyimide. After exposure and development, the sample is sputter-coated with Au–Pd. The sample is embedded in an epoxy, and then sliced with a diamond-knife microtome. The layers of PMMA shown in Fig. 2 may be somewhat thicker than the PMMA layers used with Si substrates; also, the e-beam used for this exposure is more diffuse than the beam used for high-resolution exposures, due to the larger field size and higher beam current employed. In any case, the undercut nature of the profile is clearly evident. Figure 3 shows a test pattern of Au on an oxidized Si substrate. The lines shown in Fig. 3 are 45 nm wide, with a 150 nm pitch. This pattern indicates that the lateral extent of the undercut cannot be more than ~50 nm from the resist edge.

The undercut resist profiles achieved with the bilayer resist are particularly useful for certain materials such as aluminum, which apparently migrate over the resist edges during evaporation. In contrast, materials such as chrome and gold can be patterned easily with thin ($\lesssim$ 100 nm) single-layer PMMA resist. Sputtered materials (i.e., Nb, Ta, or W) also require a strongly undercut resist profile, since sputter deposition is not highly directional.

We may compare our results with those of other workers. With the same PMMA/PMMA bilayer approach, Mackie and Beaumont[5] have achieved narrower minimum linewidths (10 nm). Their beam size was ~8 nm, as determined in a transmission measurement; this appears to be smaller than our beam size. Their smaller beam size results from their use of higher beam energy, and from their ability to focus and stigmate in the transmission mode.

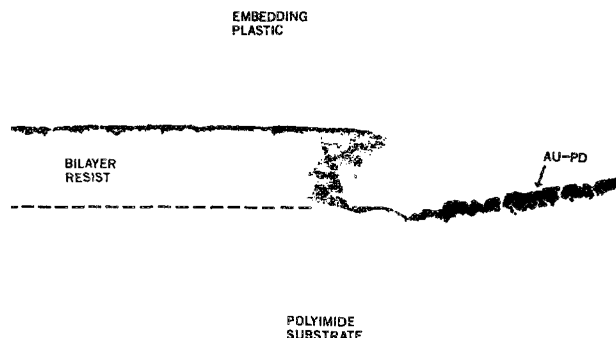

FIG. 2. TEM micrograph of the PMMA/PMMA bilayer resist profile. The bilayer is spun on a substrate of polyimide. After exposure and development the sample is coated with Au–Pd, then embedded in epoxy. Thin samples are prepared by slicing with a microtome. The resist used for this sample may be somewhat thicker than the resist used for Si substrates (Fig. 1).

With a PMMA/copolymer bilayer, Howard and coworkers have reported a minimum linewidth of 35 nm in early work using an SEM exposure system. That linewidth, like ours, was most likely limited by the exposure tool. In later studies,[4] STEM exposure of single-layer PMMA on a thick substrate allowed liftoff patterning of 10 nm Au–Pd lines. The PMMA copolymer bilayer has an advantage relative to our PMMA/PMMA bilayer that one can use mutually exclusive developers, which allows better control of the amount of undercut, especially for large undercuts. However, for achieving the more vertical liftoff profiles needed for dense patterns, the PMMA/PMMA bilayer may be preferable since only one development time needs to be tightly controlled.

The contamination resist patterning method has demon-

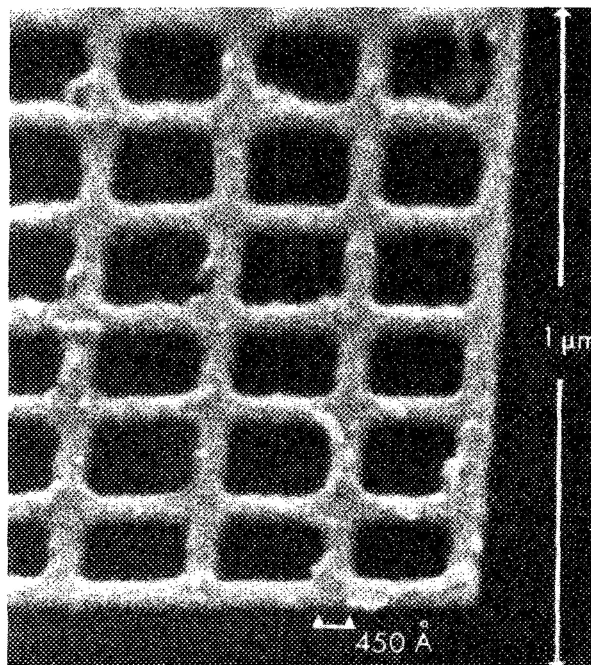

FIG. 3. Pattern of Au on oxidized Si wafer. Linewidth is 45 nm, and repeat distance is 150 nm. Liftoff was used; the mechanical integrity of the small resist structures is indicated by this liftoff pattern.

strated resolution below 10 nm.[14] In this method vacuum pump oil is hardened on a metal film surface by e-beam exposure and serves as a mask for Ar–ion etching. STEM exposure has been used with thin membrane substrates.[14] This allows a very small beam size, and facilitates focusing. However, substrate size is limited, and a separate metal layer for electrical contact pads may need to be patterned prior to the deposition of the device film. If one uses the same film for the contact pads and the device, the patterning of the pads may pose problems for a few materials. With an Ag film, for example, baking the PMMA resist (which is used as an etch mask to define large area structures) causes voids to form in the Ag film.[15] This can produce difficulties in quantum-transport experiments. For such materials, liftoff processing is preferable. Contamination resist also requires very heavy exposure. Contamination resist is, however, well suited for patterning refractory devices, such as Nb micro-SQUIDs,[2] and has been very successful for this and for experiments on quantum transport in Au rings.[9(a)]

V. SCIENTIFIC STUDIES

At Yale University e-beam lithography has been used to produce a variety of devices for physics studies. The low-temperature magnetoresistance of Al and Ag wires as narrow as 40 nm has been measured [16] to determine the electron phase-breaking rate. These wires are narrower than the thermal quantum diffusion length,[8(a)] $(\hbar D/k_B T)^{1/2}$, with D the diffusion constant, so that one observes an electron phase-breaking rate which corresponds to one-dimensional electron–electron scattering with small energy transfers.[17] This type of scattering is the dominant mechanism for energy loss in such small wires, and defines the relevant dimensional length scale. These wires and wider wires ($\gtrsim 0.1\ \mu$m) have also been used to study electron localization effects which arise from quantum interference.[8(a)] More explicit quantum interference effects are seen in small rings (1 or 2 μm diameter) of Al and Ag.[8(b)] An example of such a ring is shown in Fig. 4. The resistance of these rings oscillates with a magnetic flux period of h/e and $h/2e$. These electron interference effects are the solid-state analog of the Aharonov–Bohm effect for electrons in vacuum. The resolution of electron beam lithography is required in this case, since the diameter of the ring must be less than or comparable to the phase-breaking length l_ϕ for electrons in the metal, with $l_\phi \lesssim 1\ \mu$m. Electron-beam lithography is now being used to produce small MOSFET structures as well as other novel device structures.

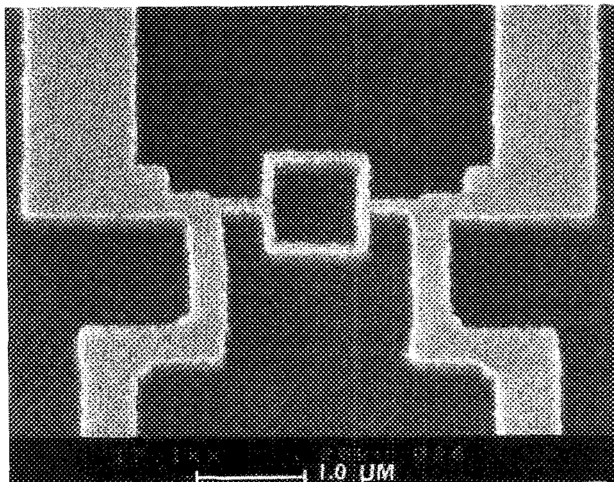

FIG. 4. Micrograph of 1 μm diam metal ring on a Si substrate with current and voltage leads.

ACKNOWLEDGMENTS

We thank R. E. Howard, S. Mackie, S. P. Beaumont, C. D. W. Wilkinson, and J. Sauvageau for helpful discussions. We also thank P. Mâle and H. Stukenbrok of the Yale Medical School for help in SEM/TEM studies. This research was supported by NSF grants ECS-8305000, ECS-8509135, and DMR-8505539. Facilities support was provided by NSF DMR-8213080, IBM Corp., Shipley, Inc., and Yale University.

[1]R. E. Howard and D. E. Prober, in *VLSI Electronics: Microstructure Science*, edited by N. E. Einspruch (Academic, New York, 1982), Vol. V, p. 145.

[2]R. B. Laibowitz and C. P. Umbach, in *Percolation, Localization, and Superconductivity*, NATO ASI Series B: Physics (Plenum, New York 1983), Vol. 109, p. 267.; W. W. Molzen, A. N. Broers, J. J. Cuomo, J. M. E. Harper and R. B. Laibowitz, J. Vac. Sci. Technol. **16**, 269 (1980).

[3]R. E. Howard, E. L. Hu, and L. D. Jackel, IEEE Trans. Electron Devices **ED-28**, 1378 (1981).

[4]H. G. Craighead, R. E. Howard, L. D. Jackel, and P. M. Mankiewich, Appl. Phys. Lett. **42**, 38 (1983); P. M. Mankiewich, R. E. Howard, L. D. Jackel, W. J. Skocpol, and D. M. Tennant, J. Vac. Sci. Technol. B **4**, 380 (1986).

[5]S. Mackie and S. P. Beaumont, Solid State Technol. **28**, 8, 117 (1985).

[6]D. C. Flanders and A. E. White, J. Vac. Sci. Technol. **19**, 892 (1981); A. C. Warren, I. Plotnik, E. H. Anderson, M. L. Schattenburg, D. Antoniadis, and H. Smith, J. Vac. Sci. Technol. B **4**, 365 (1986).

[7]D. J. Bishop, J. C. Licini, and G. J. Dolan, Appl. Phys. Lett. **46**, 1000 (1985).

[8]Examples of recent scientific studies of nm-scale devices are given in the following, in Ref. 9, and in references therein: (a) P. Santhanam, S. Wind, and D. E. Prober, Phys. Rev. Lett. **53**, 1179 (1984); (b) V. Chandrasekhar, M. J. Rooks, S. Wind, and D. E. Prober, Phys. Rev. Lett. **55**, 1610 (1985).

[9](a) R. A. Webb, S. Washburn, C. P. Umbach, and R. B. Laibowitz, Phys. Rev. Lett. **54**, 2696 (1985); (b) R. E. Howard, P. F. Liao, W. J. Skocpol, L. D. Jackel, and H. G. Craighead, Science 221, 117 (1983).

[10]B. J. Lin, in *Introduction to Microlithography*, edited by L. F. Thompson and C. G. Wilson, ACS Symposium Series **219** (American Chemical Society, 1983), p. 287.

[11]M. Hatzakis, J. Vac. Sci. Technol. **16**, 1984 (1979); W. D. Grobman, H. E. Luhn, T. P. Donohue, A. J. Speth, A. Wilson, M. Hatzakis, and T. H. P. Chang, IEEE Trans. Electron Dev. **ED-26**, 360 (1979).

[12]B. J. Lin, IBM J. Res. Dev. **20**, 213 (1976); B. J. Lin, J. Vac. Sci. Technol. **12**, 1317 (1975).

[13]UVP Inc., San Gabriel, CA (Preliminary Data Release Z-800/08/78).

[14]A. N. Broers, W. W. Molzen, J. J. Cuomo, and N. D. Wittels, Appl. Phys. Lett. **29**, 596 (1976).

[15]C. P. Umbach (private communication).

[16]S. Wind, M. J. Rooks, V. Chandrasekhar, and D. E. Prober, Phys. Rev. Lett. **57**, 633 (1986).

[17]B. L. Alt'shuler, A. G. Aronov, and D. E. Khmelnitskii, J. Phys. C **15**, 7367 (1982).